

Primary User DoA and RSS Estimation in Cognitive Radio Networks Using Sectorized Antennas

Janis Werner*, Jun Wang[†], Aki Hakkarainen*, Mikko Valkama* and Danijela Cabric[†]

* Department of Electronics and Communications Engineering
Tampere University of Technology, P.O. Box 553, FI-33101 Tampere, Finland
Emails: {janis.werner, aki.hakkarainen, mikko.e.valkama}@tut.fi

[†] Electrical Engineering Department
University of California Los Angeles, Los Angeles, CA 90095, USA
Emails: {eejwang, danijela}@ee.ucla.edu

Abstract—Received-signal-strength (RSS) and direction-of-arrival (DoA) are the sufficient measurements to solve the primary user localization problem in cognitive radio networks. In this paper we consider using energy measurements from sectorized antenna to estimate RSS and DoA of a primary user. Abstracting from practical antenna types, we define a sectorized antenna as an antenna that can be set to different operating modes, each of which resulting in a selectivity of those signals that arrive from within a certain, continuous range of angles, i.e. a sector. We first characterize the achievable performance of RSS and DoA estimations using energy measurements from sectorized antennas by means of the Cramer-Rao Bound (CRB), which provides a lower bound on the estimation accuracy of any unbiased estimator. We then propose a practical RSS and DoA estimator, namely the simplified least squares (SLS) algorithm. The SLS algorithm minimizes a cost function obtained from two largest energy measurements among all sectors, and its accuracy closely approaches the CRB. Simulation results studying the impact of important system parameters, such as SNR, number of sectors and number of samples, on the achievable accuracy specified by the CRB and the SLS algorithm are presented.

I. INTRODUCTION

Information about primary user (PU) location can enable several key capabilities in cognitive radio (CR) networks including improved spatio-temporal sensing, intelligent location-aware routing, as well as aiding spectrum policy enforcement [1]. The PU localization requires cooperation of a large amount of CRs performing passive localization, since they need to detect and localize non-cooperative PU or PUs in the whole coverage area at a very low signal-to-noise ratio (SNR) [2]. Prior research on passive localization can be categorized into three classes based on the types of measurements shared among sensors, namely received-signal-strength (RSS), time-difference-of-arrival (TDoA) and direction-of-arrival (DoA) [3]. TDoA-based algorithms are not suitable for CR applications since they require perfect synchronization among CRs. Therefore, RSS and DoA-based algorithms are the proper

The research leading to these results was financially supported by the Doctoral Programme of the President of Tampere University of Technology, the Tuula and Yrjö Neuvo Fund and the Finnish Funding Agency for Technology and Innovation (Tekes, under the project “Reconfigurable Antenna-based Enhancement of Dynamic Spectrum Access Algorithms”).

This work was also supported by the National Science Foundation under Grant No. 1117600.

choices for the PU localization problem. Furthermore, our earlier work shows DoA-based and joint RSS/DoA-based algorithms outperform RSS-based algorithms [2].

One specific challenge to the PU localization problem is the difficulty to apply the classical DoA estimation approach [4], [5]. The classical approach for DoA estimation assumes each sensor is equipped with an antenna array that includes a separate receiver chain for all antenna branches. The samples from all branches are then digitally processed by array processing algorithms such as MUSIC [4] and ESPRIT [5] to obtain DoA estimates. However, considering the large network size of the CR network, CR sensors should be portable and cheap devices with limited hardware and computation capability. Therefore, the cost of the antenna arrays and the complexity of array processing algorithms may make it impractical to apply the classical DoA estimation approach in CR networks.

In this paper we address low-cost and low-complexity DoA estimation using sectorized antennas. We define a sectorized antenna as an antenna structure that can be set to selectively receive energy from different sectors. Thereby, a sector denotes a continuous range of angles and selectivity means that signals, arriving from outside of the activated sector, are strongly attenuated. We further assume that sectorized antennas have unique reception capabilities, i.e. only a single sector can be activated at a time. Examples of antenna structures that can be used as sectorized antennas are switched-beam systems (SBSs) and leaky-wave antennas (LWAs). An SBS consists of an antenna array and a beamforming network that can be configured to activate one of several fixed beam patterns [6], [7]. The SBS is more suitable for CR devices since the antenna branches are combined in the RF stage and several key receiver components, such as the analog-to-digital converters, are required for only the combined signal branch, compared to having one for each antenna branch like in case of the digital antenna array [6]. An LWA [8] consists of a single antenna whose electrical properties can be modified such that the antenna’s beam is steered to the desired direction, which makes it a very promising candidate for DoA estimation in portable devices. In terms of our definition of sectorized antennas, different beams of SBSs and LWAs can be used to achieve the selectivity in each of the sectors.

For DoA estimation using sectorized antennas, the prior work requires knowledge of RSS or additional hardware cost. A DoA estimation algorithm based on neural networks is proposed in [7] for multiple DS-CDMA signals impinging on a base station equipped with an SBS. However, the algorithm requires either the RSS to be known or an additional, nearly omnidirectional, antenna at the receiver that is used to normalize the received energies properly. Analog DoA estimation using an LWA is presented in [9]. However, it is based on continuously changing the antenna's beam, i.e. scanning the received energy as a function of the angle, instead of measurements in sectors.

In this paper, we consider digital signal processing (DSP)-based DoA estimation algorithms using sectorized antennas, that are independent of the underlying technology, as well as the achievable performance of such algorithms. We first formulate the Cramer-Rao Bound (CRB) for RSS and DoA estimates obtained from energy measurements of sectorized antennas. The CRB provides a lower bound on the estimation accuracy of any unbiased estimator. We then propose a practical algorithm, namely the simplified least square algorithm (SLS), for RSS and DoA estimation. The SLS algorithm exploits the fact that for any given DoA, only a few sectors contain considerable signal energy, if the antenna pattern is adequately selective. Therefore, the SLS algorithm formulates the RSS and DoA estimation as a least square problem using only the two largest energy measurements from all sectors. In general a grid search can then be used to estimate DoA and RSS. However, we also derive a closed-form solution for those antennas that can be approximated using a Gaussian radiation pattern. The SLS algorithm provides a better estimation accuracy than the MaxE algorithm, which is a simple RSS and DoA estimator we proposed in our early work [10], and closely approaches the CRB. Simulation results studying the impact of important system parameters, such as SNR, number of sectors and number of samples, on the achievable accuracy and the SLS algorithm are presented.

The rest of the paper is organized as follows. The system model is introduced in Section II. The CRB for DoA and RSS estimates obtained from sectorized antennas is presented in Section III. The RSS and DoA estimation algorithms are formulated in Section IV. Numerical results evaluating the impact of various parameters on DoA and RSS estimators and the CRB are discussed in Section V. Finally, the paper is concluded in Section VI.

II. SYSTEM MODEL

In this paper we consider a CR device estimating the DoA and RSS of a PU signal without any detailed information about the transmission. On that account, the CR is equipped with an antenna whose properties can be modified such that measurements in M different sectors are possible. Thereby, sectors are characterized by the radiation pattern, which describes the attenuation of the PU signal as a function of its DoA. In this paper we first develop the CRBs and algorithms in a general form such that they are applicable to any sectorized antenna.

However, in order to identify some general trends, we then assume that the radiation pattern, $p(\varphi - \vartheta_m)$, depends only on the angular distance between the PU signal's DoA, φ , and orientation ϑ_m of sector m , $m = 1 \dots M$. In addition, for analysis purposes, we further simplify the model of the radiation pattern by approximating only the antenna's main beam using a Gaussian-like shape as proposed in [11]. Then, the radiation pattern can be expressed as

$$p(\varphi) = \exp\left(-[\mathcal{M}(\varphi)]^2/\beta\right) \quad (1)$$

where $\mathcal{M}(\varphi) = \text{mod}_{2\pi}(\varphi + \pi) - \pi$ is used to restrict the input angle to $[-\pi, \pi]$ and β is a parameter determining the width of the beam. The spacing between the sectors, $\Delta\vartheta = \frac{2\pi}{M}$, is assumed to be constant, such that the orientation of sector m becomes $\vartheta_m = m\Delta\vartheta$. Instead of parameterizing the radiation pattern via the beamwidth, we use a value that we denote the side-sector suppression, a_s . We define the side-sector suppression as the attenuation that a signal, arriving at the orientation ϑ_m of the m^{th} sector, experiences in the neighboring sectors $m-1$ and $m+1$, i.e. $a_s = p(\Delta\vartheta)$. Therefore, the side-sector suppression determines the amount of overlap between neighboring sectors, independent of the number of sectors. The result is a beamwidth determined by

$$\beta = -(2\pi)^2 [M^2 \ln(a_s)]^{-1}. \quad (2)$$

During the measurement period, the CR successively switches through the M sectors and receives N complex samples for each sector, which results in $M \times N$ complex samples in total. Then, the baseband complex received signal sample originating from the m -th sector, with the sample index range $n = (m-1)N + 1 \dots mN$, can be written as

$$x(n) = p(\varphi - \vartheta_m) s(n) + w(n), \quad (3)$$

where $w(n) \sim \mathcal{CN}(0, \sigma_w^2)$ is additive noise assumed to be circular symmetric complex Gaussian. Likewise, the noiseless part of the received PU signal is modeled as circular symmetric complex Gaussian, i.e. $s(n) \sim \mathcal{CN}(0, \gamma)$, which is a good approximation for e.g. OFDM-based transmission.

Given the above stated assumptions, it is impossible to distinguish between the PU signal and noise at the CR. Therefore, the estimations of RSS γ and DoA φ should be based on the received energies. The power in sector m is calculated according to

$$\epsilon_m = \frac{1}{N} \sum_{n=(m-1)N+1}^{mN} |x(n)|^2, \quad (4)$$

resulting in chi-squared distributed values ϵ_m with $2N$ degrees of freedom. For moderate to large values of N , the energies can therefore be well approximated using a Gaussian distribution (see e.g. [12]), i.e. $\epsilon_m \sim \mathcal{N}(\mu_m, \sigma_m^2)$, with the parameters

$$\mu_m = \sigma_w^2 + \rho_m \gamma \quad (5)$$

$$\sigma_m^2 = \frac{1}{N} (\sigma_w^2 + \rho_m \gamma)^2 \quad (6)$$

where $\rho_m = [p(\varphi - \vartheta_m)]^2$.

III. CRAMER-RAO BOUNDS

The CRB is a lower bound on the covariance matrix of any unbiased estimator. For the estimation of a $K \times 1$ parameter vector \mathbf{r} , given the $L \times 1$ vector $\boldsymbol{\epsilon}$ composed of the observations, the CRB is obtained as the inverse of the Fisher information matrix (FIM). The FIM is element-wise defined as

$$\mathbf{F}_{i,j} = -\mathbf{E} \left(\frac{\partial^2}{\partial \mathbf{r}_i \partial \mathbf{r}_j} \ln [f(\boldsymbol{\epsilon}|\mathbf{r})] \right), \quad i, j = 1 \dots K \quad (7)$$

where $f(\boldsymbol{\epsilon}|\mathbf{r})$ is the posterior probability distribution of $\boldsymbol{\epsilon}$ given \mathbf{r} .

Here, $K = 2$ since we estimate $\mathbf{r} = [\varphi, \gamma]^T$, using the $L = M$ energies $\boldsymbol{\epsilon} = [\epsilon_1, \epsilon_2, \dots, \epsilon_M]^T$. Given the Gaussian approximation of the energy distribution, (5) and (6), the posterior probability distribution becomes

$$f(\boldsymbol{\epsilon}|\mathbf{r}) = \frac{1}{(2\pi)^{\frac{M}{2}} |\mathbf{Q}|^{\frac{1}{2}}} \exp \left\{ -\frac{1}{2} (\boldsymbol{\epsilon} - \mathbf{g})^T \mathbf{Q}^{-1} (\boldsymbol{\epsilon} - \mathbf{g}) \right\} \quad (8)$$

with $\mathbf{g} = [\mu_1, \mu_2, \dots, \mu_M]^T$ and $\mathbf{Q} = \text{diag} [\sigma_1^2, \sigma_2^2, \dots, \sigma_M^2]$. In this paper we only present the final result for the resulting FIM while the detailed derivation, that will be part of a more extensive journal article, can be found in [13]. With the SNR = $\frac{\gamma}{\sigma_w^2}$, the elements of the FIM can be expressed as

$$\mathbf{F}_{11} = (N+2) \sum_{m=1}^M \frac{\tilde{\rho}_m^2}{(\rho_m^{-1} \text{SNR}^{-1} + 1)^2} \quad (9)$$

$$\mathbf{F}_{12} = \mathbf{F}_{21} = \frac{(N+2)}{\gamma} \sum_{m=1}^M \frac{\tilde{\rho}_m}{(\rho_m^{-1} \text{SNR}^{-1} + 1)^2} \quad (10)$$

$$\mathbf{F}_{22} = \frac{(N+2)}{\gamma^2} \sum_{m=1}^M \frac{1}{(\rho_m^{-1} \text{SNR}^{-1} + 1)^2}. \quad (11)$$

Thereby, the value of $\tilde{\rho}_m = \frac{[\rho_m]_\varphi}{\rho_m}$ is a function of the radiation pattern and its derivative with respect to the DoA, i.e. $[\rho_m]_\varphi$. For the Gaussian radiation pattern (1), $\tilde{\rho}_m$ is equal to $\tilde{\rho}_m = -4\mathcal{M}(\varphi - \vartheta_m) / \beta$. Finally, we obtain the following relations for the lower bound on the root mean square error (RMSE) of DOA estimation

$$\text{RMSE } \hat{\varphi} \geq \sqrt{[\mathbf{F}^{-1}]_{11}} \quad (12)$$

and on the relative RMSE (RRMSE) of RSS estimation

$$\text{RRMSE } \hat{\gamma} = \frac{\text{RMSE } \hat{\gamma}}{\gamma} \geq \frac{\sqrt{[\mathbf{F}^{-1}]_{22}}}{\gamma} \quad (13)$$

that we have normalized to be independent of the RSS.

IV. DOA AND RSS ESTIMATORS

A. MaxE Estimator

A rough estimate of the DoA and RSS can be obtained using the following intuitive estimator that we refer to as the MaxE estimator [10]. The MaxE estimator finds the maximum power and uses the orientation of the associated sector as the DoA

estimate, while the RSS estimate is obtained by subtracting the noise variance from the maximum energy:

$$\hat{\varphi}_m = \{\vartheta_i \mid i = \arg \max_i \epsilon_i\} \quad (14)$$

$$\hat{\gamma}_m = \max_i \epsilon_i - \sigma_w^2. \quad (15)$$

It is easily verified that the resulting estimates are biased. Therefore, the performance of the MaxE estimator cannot be compared to the CRB. However, since the computational complexity of the MaxE estimator is very low, it serves anyway as a practical performance benchmark for more advanced estimators.

B. Proposed Simplified Least Squares Estimator

Using the same notation as in Sec. III, the received energies can be written in vector-form as

$$\boldsymbol{\epsilon} = \mathbf{g}(\varphi, \gamma) + \mathbf{e}, \quad (16)$$

where \mathbf{e} is an $M \times 1$ random vector that is independent of the RSS and DoA. In the LS approach the RSS and DoA estimates are then estimated such that the LS error criterion,

$$J(\varphi, \gamma) = [\boldsymbol{\epsilon} - \mathbf{g}(\varphi, \gamma)]^T [\boldsymbol{\epsilon} - \mathbf{g}(\varphi, \gamma)], \quad (17)$$

is minimized. However, $\mathbf{g}(\varphi, \gamma)$ is nonlinear in φ and γ . Therefore, the minimization of (17) requires iterative algorithms whose convergence depends on the initial guess and is not guaranteed. Intuitively, the energy measurements indicate the contribution that each sector has in the RSS and DoA estimation process. If the sectorized antenna exhibits good directionality, if the SNR is at a practical level (above 0 dB) and if the number of samples is finite, then the PU signal component, i.e. $\rho_m \gamma$, is of meaningful strength only in very few sectors, while the remaining measurements are too noisy to exploit their PU signal component. Let $r = (r_1, r_2 \dots r_M)$ denote a permutation such that $\epsilon_{r_1} < \epsilon_{r_2} < \dots < \epsilon_{r_M}$. Then, the PU signal DoA is most likely in-between the sectors with the highest energy, i.e. $\vartheta_{r_M} < \varphi < \vartheta_{r_{M-1}}$. Sectors r_M and r_{M-1} also contribute most to the DoA and RSS estimation. Therefore, a good approximation of the LS solution is obtained by finding the DoA $\hat{\varphi}_{\text{SLS}}$ that minimizes

$$J_{\text{SLS}} = \left(\overline{\Delta \epsilon} - \frac{\rho_{r_M}}{\rho_{r_{M-1}}} \right)^2 \quad (18)$$

with

$$\overline{\Delta \epsilon} = \frac{\epsilon_{r_M} - \sigma_w^2}{\epsilon_{r_{M-1}} - \sigma_w^2} = \frac{\rho_{r_M} \gamma + e_{r_M}}{\rho_{r_{M-1}} \gamma + e_{r_{M-1}}}. \quad (19)$$

Since (18) is independent of the RSS and the DoA is restricted to the finite interval $\varphi \in [-\pi; \pi]$, a solution may be obtained using a simple grid search. However, if the antenna's main beam can be approximated using the Gaussian pattern (1), the DoA estimate minimizing (18) can also be obtained in closed-form according to

$$\hat{\varphi}_{\text{SLS}} = \frac{\frac{1}{2} \beta \ln \overline{\Delta \epsilon} + \vartheta_{r_M}^2 - \vartheta_{r_{M-1}}^2}{2(\vartheta_{r_M} - \vartheta_{r_{M-1}})}. \quad (20)$$

Note that the closed-form solution (20) is also applicable to antennas whose main beams differ in every sector, as long as all of them may be approximated by the Gaussian radiation pattern. In that case the parameter β in (20) is sector-dependent. An estimation of the attenuation in each of the sectors follows directly from the estimated DoA, according to $\hat{\rho}_m = [p(\hat{\varphi}_{\text{SLS}} - \vartheta_m)]^2$. As a consequence, an RSS estimate can be calculated for each of the sectors. In order to reduce the effect of statistical fluctuations, we then obtain a final estimate of the RSS by averaging over the RSS estimates from the two sectors with the highest energies, i.e.

$$\hat{\gamma}_{\text{SLS}} = \frac{1}{2} [(\epsilon_{r_M} - \sigma_w^2) / \hat{\rho}_M + (\epsilon_{r_{M-1}} - \sigma_w^2) / \hat{\rho}_{M-1}]. \quad (21)$$

In the following we refer to the algorithm that estimates the DoA based on the minimization of (18) and the respective RSS estimation (21) as the SLS estimator. In order to prevent large estimation errors when the signal is severely attenuated, we have added a validation check that reduces the SLS to the MaxE algorithm in the following cases:

- 1) If $\epsilon_{r_{M-2}} < \sigma_w^2$ then DoA estimation is according to (14).
- 2) If the estimated angle, $\hat{\varphi}_{\text{SLS}}$, is not in-between the two sectors with the highest energies then RSS estimation is according to (15).

V. SIMULATION RESULTS

The bounds and algorithms for DoA and RSS estimation are studied assuming a uniform distribution of incoming DoAs, i.e. $\varphi \sim \mathcal{U}(-\pi; \pi)$. We emulate this distribution via 10^2 equidistant steps in the interval $\varphi_k \in [-\frac{\Delta\vartheta}{2}; \frac{\Delta\vartheta}{2}]$, and simulate 10^3 realizations per algorithm and DoA-step, and average over the result at each step in order to obtain the RMSE and absolute value of bias (AB). The CRB on the RMSE of DoA estimation (12) and the CRB on the RRMSE of RSS estimation (13) depend only on the SNR, not on the RSS. The same conclusion applies for the algorithms presented in Sec. IV. Therefore, we set the RSS to a fixed value $\gamma = 1\text{pW}$ and adjust the noise power σ_w^2 in order to control the SNR.

Fig. 1 shows the dependence of DoA estimation performance on the side-sector suppression a_s . For high values of $a_s \approx 1$, the antenna is close to omnidirectional and as a consequence, DoA estimation becomes impossible and the RMSE is very high. This trend, observed for the CRB as well as the algorithms, is very intuitive. However, if the side-sector suppression is too low, the RMSE for the CRB and algorithms is also high. In order to understand this behavior, we consider Fig. 2, which depicts the DoA estimation RMSE as a function of the incoming DoA. Since we assume the same radiation pattern for all sectors and since the assumed Gaussian radiation pattern (1) is symmetric with respect to $\varphi = 0$, the resulting RMSE curves are periodic with the period $\Delta\vartheta$ and it is sufficient to consider the normed DoA, $\varphi' = \frac{\varphi}{\Delta\vartheta}$, over the finite interval $\varphi' \in [0; 0.5]$. Then, the value $\varphi' = 0$ represents all DoAs that arrive at the orientation ϑ_m of a sector $m = 1 \dots M$, while $\varphi' = 0.5$ represents DoAs that arrive in-between two sectors. For the sake of clarity we have

not added the curves of MaxE estimation to Fig. 2. However, due to its simplicity it is easy to see that the RMSE of the MaxE estimator increases with φ' . This is explained by the discretization of $\varphi \in [-\pi; \pi]$ to $\hat{\varphi} \in \{\vartheta_m | m = 1 \dots M\}$ as well as due to the attenuation of signals that is increasing with φ' . This signal attenuation, which is stronger for smaller a_s , explains the high RMSE resulting from MaxE estimation in combination with low values of a_s in Fig. 1. With respect to the CRB, on the other hand, the RMSE decreases with φ' . This is due to the estimation of the DoA that is dependent on the shape of the radiation pattern, which has its lowest slope ($=0$) at the orientation of a sector. With a low slope, small variations in the measured energies appear as big changes of the DoA, while the pattern's high slope at around $\varphi' \approx 0.5$ makes the DoA estimation more stable towards variations in the measured energies. For a medium value a_s , information not only from the sector at which the signal is arriving, but also from the neighboring sectors is available, resulting in a more even distribution of the RMSE over the whole DoA range. Due to the validity checks discussed in Sec. IV-B, the behavior of SLS estimation depends on the operating conditions. Whenever the operating conditions are disadvantageous for the estimation, it is likely that the validity checks result in the reduction of SLS to MaxE. As observed in Fig. 1, the quality of operating conditions for estimation and therefore the reduction of SLS to MaxE is, among other parameters, influenced by a_s . As discussed in Sec. IV-A, the MaxE algorithm is biased and therefore not necessarily bounded by the CRB, which is a lower bound only on unbiased estimators. As a consequence, SLS estimation in disadvantageous operating conditions is also biased and therefore not always lower bounded by the CRB either, as can be seen in Fig. 1 and Fig. 2 (note, that SLS is biased as soon as $\text{AB} \neq 0$ for any $\varphi/\Delta\vartheta$) for low values of a_s . However, for moderate values of a_s , the bias of SLS is close to zero. Then, we observe in Fig. 2 a behavior similar to that of the CRB, i.e. the RMSE decreases with φ' .

Fig. 3 depicts the RRMSE of RSS estimation as a function of a_s . For RSS estimation, performance increases with a_s , i.e. the more the radiation pattern resembles that of an omnidirectional antenna. An exception is the small positive slope in the RRMSE of MaxE and SLS estimation for very large values of a_s . As a practical guideline, we would like to determine the value, $a_{s,o}$, of the side-sector suppression that results in the lowest RMSE for both DoA and RSS estimation in relevant operating conditions. However, we have seen that the best performance of DoA estimation is achieved for a medium value of a_s , while best performance of RSS estimation is, at least from the theoretical point of view, achievable for $a_s \approx 1$. With respect to the CRB on DoA estimation, the value $a_{s,o}$ seems to be independent of the parameters M and N . Merely an increase of the SNR results in a small shift of $a_{s,o}$ towards a more directional antenna. With respect to the algorithms on the other hand, not only increasing the SNR but also a decrease of M results in a shift of $a_{s,o}$ towards smaller values. Overall, the value $a_s = 0.4$ has proven to be a good tradeoff between RSS and DoA estimation and is henceforth

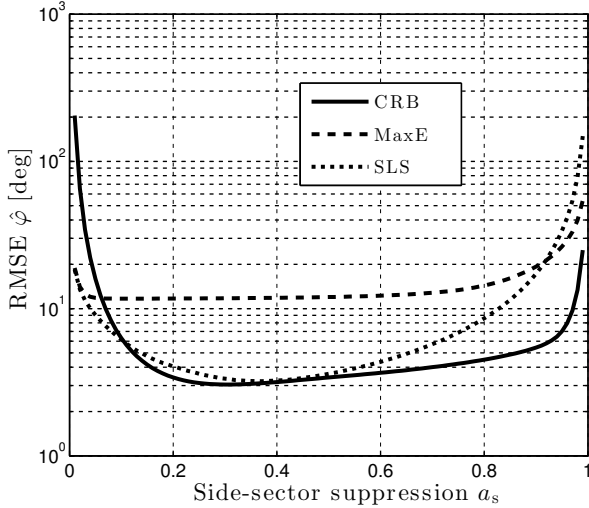


Fig. 1. Performance of DoA estimation as a function of the side-sector suppression for a uniform distribution of DoAs. Parameters: $M = 9$, $N = 50$, SNR = 5 dB.

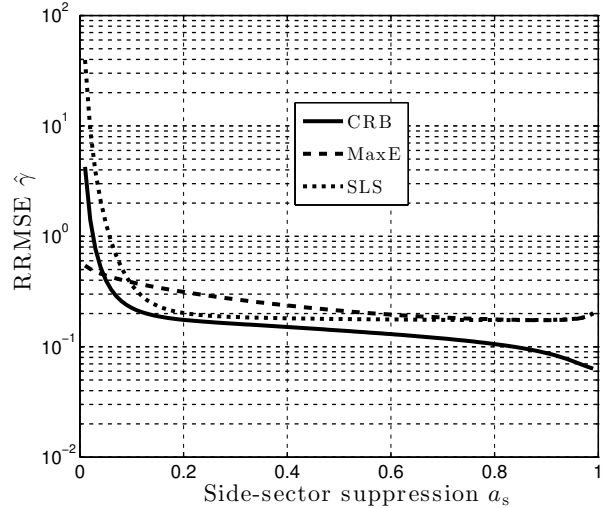


Fig. 3. Performance of RSS estimation as a function of the side-sector suppression for a uniform distribution of DoAs. Parameters: $M = 9$, $N = 50$, SNR = 5 dB.

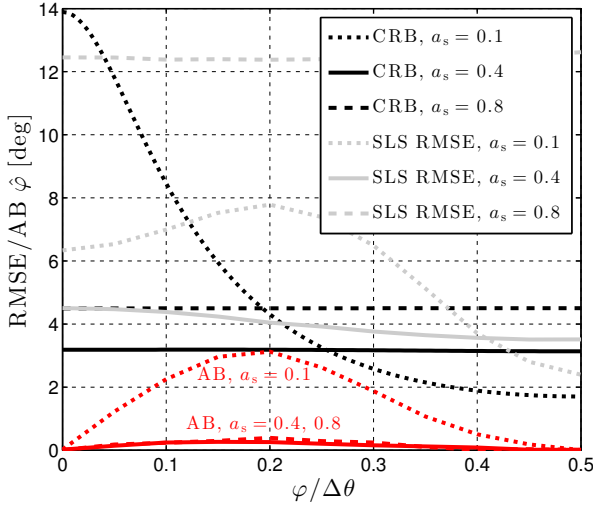


Fig. 2. Dependence of DoA estimation on the incoming DoA. Parameters: $M = 9$, $N = 50$, SNR = 5 dB.

used as the default value. Fig. 4 and Fig. 5 show the influence of the SNR on the DoA and RSS estimation performance. Since the SNR also influences the operating conditions for estimation and as a consequence the bias of SLS estimation, Fig. 4 and Fig. 5 depict the AB/relative AB ($\text{RAB } \hat{\gamma} = \text{AB}/\gamma$) along with the RMSE/RRMSE. As expected, the CRBs and the RMSE/RRMSE of SLS estimation decrease with increasing SNR. Furthermore, we observe that the SLS yields biased DoA and RSS estimates for SNR values that are smaller than 5 dB. However, very low SNR values have little practical relevance as they make it difficult to detect the PU signal in the first place [12]. Thus, for most of the practical relevant cases and a well parameterized antenna ($a_s \approx 0.4$) the SLS algorithm is unbiased and therefore lower bounded by the CRB. In contrast to the behavior observed in CRB and SLS estimation, the RMSE and RRMSE of MaxE estimation decrease only up to SNR ≈ 5 dB. For an SNR > 5 dB the performance is

constant due to the bias in the estimation [10]. In case of DoA estimation, the performance of the MaxE estimator is significantly worse than the CRB. While the RMSE of SLS-based DoA estimates is larger than the CRB, the algorithm always results in a smaller RMSE than the MaxE estimator. For an SNR = -2 dB, the difference between the MaxE and SLS RMSE is only $\approx 5^\circ$. Performance starts to differ significantly from an SNR ≈ 0 dB onwards. Then, the MaxE RMSE does not decrease anymore, while the SLS estimator starts to perform close to the CRB (1° difference at 5 dB). This coincides also with the level of SNR where the SLS algorithm starts to yield almost unbiased DoA estimates. For RSS estimation, the MaxE and SLS estimator have a lower RRMSE than the CRB if the SNR is very low (< -1 dB), i.e. an SNR region where both algorithms were biased. Otherwise, MaxE estimation results in the largest RMSE while the RMSE of SLS estimation is only slightly larger than the CRB.

Finally, Fig. 6 depicts the estimation performance as a function of the number of samples N and with two different numbers of sectors $M \in \{5, 9\}$. Since the dependence of RSS and DoA estimation on N is very similar, we chose to include only the curve for DoA estimation in this paper. As with the SNR, an increase of N results in a smaller SLS-RMSE and a lower CRB, while the performance of MaxE estimation saturates for comparably low N and at a high RMSE. Again, the CRB is lower than the RMSE of the estimators, while SLS is outperforming the MaxE estimator significantly. An increase of M is always beneficial for DoA estimation. In contrast to this, the RSS RRMSE is almost independent of M since the attenuation in neighboring sectors is constant due to the parametrization via (2), such that only a limited amount of sectors contribute to RSS estimation anyways.

VI. CONCLUSION

We considered the problem of estimating RSS and DoA of the primary user in cognitive radio networks using energy mea-

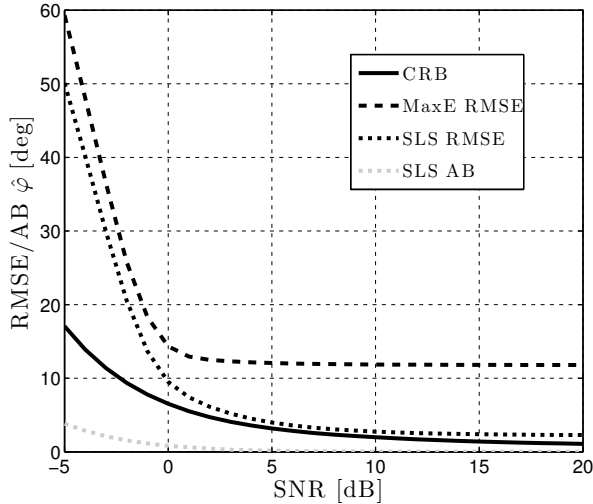


Fig. 4. Performance and bias of DoA estimation as a function of the SNR for a uniform distribution of DoAs. Parameters: $a_s = 0.4$, $M = 9$, $N = 50$.

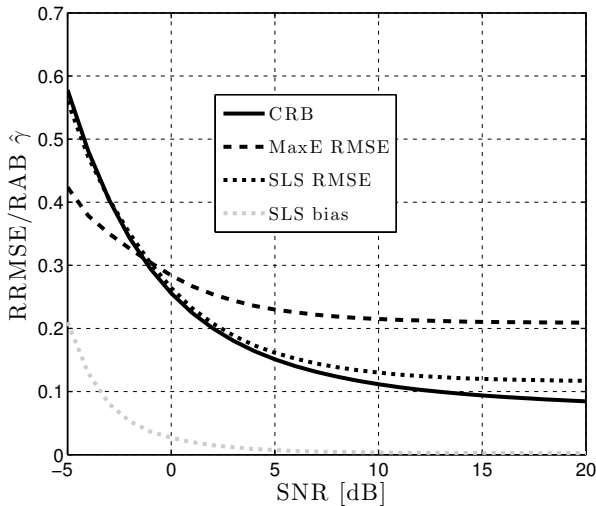


Fig. 5. Performance and bias of RSS estimation as a function of the SNR for a uniform distribution of DoAs. Parameters: $a_s = 0.4$, $M = 9$, $N = 50$.

measurements from sectorized antennas. We first formulated the CRBs for such problem, which provides the lower bound on the achievable accuracy of any unbiased estimators. We then proposed the SLS algorithm, which is a simple estimator based on the two largest energy measurements among all antenna sectors. Simulation results of the impact of various important system parameters, such as side-sector suppression, number of antennas and samples, and SNR, on the CRB and SLS algorithm were presented to provide guidelines for practical systems and algorithm design. Our results showed that the SLS algorithm closely approaches the CRB for positive SNR values and also outperforms the simple MaxE reference algorithm. Overall, the obtained results indicate that sectorized antenna systems can be used for accurate PU DoA and RSS estimation, and thereon for PU localization, in fairly low-complexity SU devices, compared to e.g. classical digital antenna arrays.

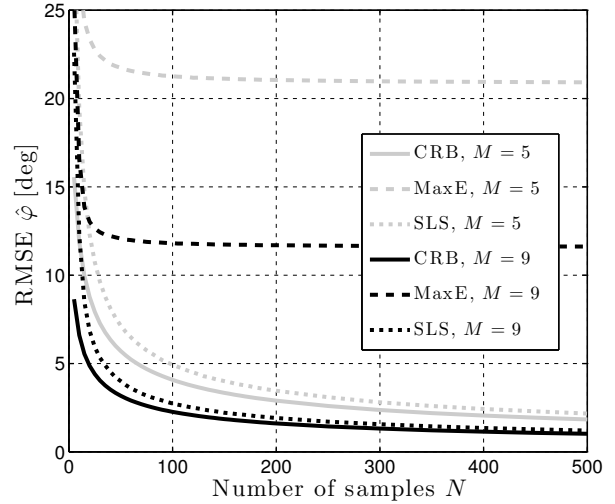


Fig. 6. Performance of DoA estimation as a function of the number of samples for a uniform distribution of DoAs. Parameters: $a_s = 0.4$, SNR = 5 dB.

REFERENCES

- [1] H. Celebi and H. Arslan, "Utilization of location information in cognitive wireless networks," *IEEE Wireless Commun. Mag.*, vol. 14, no. 4, pp. 6–13, Aug. 2007.
- [2] J. Wang, J. Chen, and D. Cabric, "Cramer-rao bounds for joint rss/doa-based primary-user localization in cognitive radio networks," *accepted for publication in IEEE Trans. Wireless Commun.*, December 2012, [Online] <http://arxiv.org/abs/1207.1469>.
- [3] N. Patwari, J. Ash, S. Kyperountas, A. Hero, R. Moses, and N. Correal, "Locating the nodes: cooperative localization in wireless sensor networks," *IEEE Signal Process. Mag.*, vol. 22, no. 4, pp. 54–69, July 2005.
- [4] P. Stoica and N. Arye, "Music, maximum likelihood, and cramer-rao bound," *IEEE Trans. Acoust., Speech, Signal Process.*, vol. 37, no. 5, pp. 720–741, May 1989.
- [5] R. Roy and T. Kailath, "Esprit-estimation of signal parameters via rotational invariance techniques," *IEEE Trans. Acoust., Speech, Signal Process.*, vol. 37, no. 7, pp. 984–995, Jul. 1989.
- [6] T. Ohira, "Adaptive array antenna beamforming architectures as viewed by a microwave circuit designer," in *Asia-Pacific Microwave Conference*, 2000, pp. 828–833.
- [7] K. Gotsis, K. Siakavara, and J. Sahalos, "On the direction of arrival (DoA) estimation for a switched-beam antenna system using neural networks," *IEEE Trans. Antennas Propag.*, vol. 57, no. 5, pp. 1399–1411, May 2009.
- [8] D. Piazza, D. Michele, and K. Dandekar, "Two port reconfigurable crlh leaky wave antenna with improved impedance matching and beam tuning," in *3rd European Conference on Antennas and Propagation 2009 (EuCAP09)*, Mar. 2009, pp. 2046–2049.
- [9] S. Abielmona, H. Nguyen, and C. Caloz, "Analog direction of arrival estimation using an electronically-scanned CRLH leaky-wave antenna," *IEEE Trans. Antennas Propag.*, vol. 59, no. 4, pp. 1408–1412, Apr. 2011.
- [10] J. Werner, J. Wang, A. Hakkarainen, M. Valkama, and D. Cabric, "Primary user localization in cognitive radio networks using sectorized antennas," *10th Annual Conference on Wireless On-Demand Network Systems and Services (WONS2013)*, Jan. 2013.
- [11] R. Martin and R. Thomas, "Algorithms and bounds for estimating location, directionality, and environmental parameters of primary spectrum users," *IEEE Trans. Wireless Commun.*, vol. 8, no. 11, pp. 5692–5701, Nov. 2009.
- [12] R. Tandra and A. Sahai, "SNR walls for signal detection," *IEEE Journal of Selected Topics in Signal Processing*, vol. 2, no. 1, pp. 4–17, Feb. 2008.
- [13] J. Werner, "Technical report." [Online]. Available: <http://www.cs.tut.fi/~%7Ewerner/ccrb/sector-crb.pdf>